Powerful helicity inducers: axially chiral binaphthyl derivatives

Munju Goh[a]; Kazuo Akagi[a]

[a] Department of Polymer Chemistry, Kyoto University, Katsura, Kyoto 615-8510, Japan

PLEASE SCROLL DOWN FOR ARTICLE

Taylor & Francis
Taylor & Francis Group

Powerful helicity inducers: axially chiral binaphthyl derivatives

Munju Goh and Kazuo Akagi*

Department of Polymer Chemistry, Kyoto University, Katsura, Kyoto 615-8510, Japan

Axially chiral binaphthyl derivatives with highly twisting powers were synthesised by substituting phenylcyclo-hexyl (PCH) mesogenic moieties into 2,2′ positions or 2,2′,6,6′ positions of binaphthyl rings. The di- and tetra-substituted binaphthyl derivatives were adopted as chiral dopants to induce chiral nematic liquid crystals (N*-LCs). The helical twisting power (β_M) of tetra-substituted binaphthyl derivative, **D-3**, having direct linkages between the PCH moieties and the binaphthyl rings at the 6,6′ positions, was $449\,\mu m^{-1}$. This is ca. 2.6 times larger than that ($171\,\mu m^{-1}$) of di-substituted one, **D-1**. For systematic investigation of helical twisting power in the binaphthyl derivatives, several tetra-substituted binaphthyl derivatives (**D-2**–**D-9**) were synthesised by introducing different aromatic moieties into the 6,6′ positions of the binaphthyl rings without methylene spacer. When the substituents group changed from *p*-hexaoxyphenyl to *p*-hexaoxybiphenyl, the helical twisting powers of the binaphthyl derivatives increased from 234 to $757\,\mu m^{-1}$. Interestingly, **D-3** and **D-9** exhibited liquid crystallinity. Although the liquid crystallinity of the chiral dopant has no direct influence on the helical twisting power of the N*-LC, it plays a role in increasing the miscibility of the chiral dopant to host N-LC, leading to a raise of the upper limit in concentration of the chiral dopant. Consequently, both the high helical twisting power and the high miscibility of **D-3** allowed us to prepare a highly twisted N*-LC, the helical pitch of which is in the nano-order, e.g. 270 nm.

Keywords: chiral nematic liquid crystal; chiral dopant; binaphthyl derivative; helical twisting power

1. Introduction

Chiral nematic liquid crystals (N*-LCs) have been attracting substantial interest for their potential applications for circularly polarised light (*1*), reflect-able polarisers (*2*), LC lasers (*3*), asymmetric synth-esis (*4*) and chirality induction for conducting polymers (*5, 6*). There are many kinds of chiral LC phase, i.e. cholesteric or N*, blue phases (*7*) and twist grain boundary (TGB) phases (*8*). In particular, the N*-LC phase can be easily induced by adding a small amount of chiral compound as a chiral dopant into a nematic LC (N-LC). The helical pitch of the N*-LC can be easily adjusted by changing the concentration of chiral dopant or by modifying the helical twisting power (HTP) of the chiral dopant itself (*9*). Most of chiral dopants have no liquid crystallinity and relatively large molecular weights. It follows that an addition of large amount of the chiral dopant to the host N-LC causes a lowering of phase transition temperature from an isotropic to a nematic phase and an increase in viscosity of the LC, as well as an occurrence of crystallization (*10*). A chiral dopant with large HTP can prevent the degradation of the N*-LC, because the desired helical pitch can be obtained by adding a relatively small amount of chiral dopant to the host N-LC. Thus, it may be more preferable for induction of a highly twisted N*-LC to

change HTP of the chiral dopant rather than to change the concentration of the chiral dopant (*11*).

It is known that the binaphthyl derivatives have large twisting powers. This property comes from large steric repulsions between hydrogen atoms at the 8,8′ positions of the naphthyl rings (*12*). Many types of binaphthyl derivatives with different substituents in the 2,2′ positions (*5, 13*), 2,2′,6,6′ positions (*5, 14*) or 2,2′,5,5′,6,6′ positions (*15*) have been examined for usages of chiral dopants to induce N*-LC. In particular, binaphthyl derivatives substituted with liquid crystalline groups at the 2,2′,6,6′ positions of the binaphthyl rings exhibit good miscibility towards the host N-LC owing to their liquid crystallinities, and also they have high HTPs based on axial chirality (*5, 14b*). However, in spite of using binaphthyl derivatives with high HTPs, it was difficult to induce N*-LCs with nano-ordered helical pitches. Thus, both miscibility and high HTP are required for the effective transfer of the axial chirality of the binaphthyl derivatives to the host N-LCs.

It has been reported that the rigid aromatic sub-stituents generate large HTPs in $\alpha,\alpha,\alpha',\alpha'$-tetraaryl-1,3-dioxolan-4,5-dimethanol derivatives (Taddol), and that the HTPs increase with the rigidity of substituents (*16, 17*). In this work, to investigate an amplification of HTPs in the axially chiral binaphthyl derivatives, we introduced several rigid substituents

---

group into the 2,2′,6,6′ positions of the binaphthyl rings. Among them, the tetra-substituted binaphthyl derivative, **D-8**, which has the direct linkage between the *p*-hexaoxybiphenyl moieties and the 6,6′ positions of the binaphthyl rings, showed an extremely high HTP of $757 \, \mu m^{-1}$. The roles of HTP and liquid crystallinity of the chiral dopant in induction of highly twisted N*-LC are also discussed.

2.   Methods

All experiments were performed under argon atmosphere. Tetrahydrofuran (THF) and dichloromethane (CH_2Cl_2) were distilled prior to use. Williamson etherification and Suzuki coupling reactions were used to synthesise the chiral binaphthyl derivatives. The chemical compounds, (*R*)- and (*S*)-2,2'-dihydroxy-1,1'-binaphthyl (optical purity, 0.99), were purchased from commercially available sources. The mesogenic compounds, 4-(*trans*-4-*n*-pentylcyclohexyl)phenol (PCH500) and 4-(*trans*-4-*n*-pentylcyclohexyl)bromobenzene (PCH5Br), were purchased from Kanto Chemical Ltd.

N-LCs of phenylcyclohexane derivatives, 4-(*trans*-4-*n*-propylcyclohexyl)ethoxybenzene (PCH302) and 4-(*trans*-4-*n*-propylcyclohexyl)butoxybenzene (PCH304), as well as di-substituted binaphthyl derivatives [(*R*)-, (*S*)-2,2′-PCH506-1,1′-binaphthyl, abbreviated as (*R*)-, (*S*)-D-1] (shown in Scheme 1), were synthesised according to the method described in a previous report (*5a*). The tetra-substituted binaphthyl derivatives, **D-2**–**D-8**, were synthesised by substituting aromatic moieties into the 6,6′ positions of the binaphthyl rings without methylene spacers. Synthetic routes for the di- and tetra-substituted binaphthyl derivatives are shown in Scheme 1. The chiral binaphthyl derivative of **D-9** was synthesised by means of the previously reported procedure (*15b*). It should be mentioned that to improve the miscibility of the chiral dopant with the host N-LCs, we introduced PCH moieties into the 2,2′ positions of binaphthyl rings (**D-1**) or into the 2,2′,6,6′ position of binaphthyl rings (**D-2**, **D-3**, **D-9**).

^{1}H and ^{13}C NMR spectra were measured in $CDCl_3$ using a JEOL 270 MHz NMR spectrometer. Chemical shifts were measured in parts per million downfield from tetramethylsilane as an internal standard. The chemical properties of the compounds synthesised are described in section 5. Polarising optical microscopy (POM) observations were carried out under crossed nicols using a Nikon ECLIPSE E 400 POL polarising optical microscope equipped with a Nikon COOLPIX 950 digital camera and a Linkam TH-600PM and L-600 heating and cooling stage with

temperature control. The phase transition temperatures of the chiral dopants and the N*-LC were determined using differential scanning calorimetry (DSC, Perkin-Elmer) and a TA instrument Q100 DSC apparatus at a constant heating and cooling rate of $10°C \, min^{-1}$, where the results in the first cooling and the second heating processes were recorded. X-ray diffraction (XRD) measurements were performed with a Rigaku D-3F diffractometer, in which the X-ray power was set at 12 kW.

3.   Results and discussion

### *Mesomorphic properties of chiral dopants*

Mesomorphic properties of the binaphthyl derivatives were investigated using DSC, POM and XRD. Among the chiral dopants synthesised, **D-3** and **D-9** exhibited liquid crystallinity. The phase transition temperatures of **D-3** were as follows: G→79°C→SmX→99°C→I and Cr←52°C←SmX←63°C←I in the heating and cooling processes, respectively (Figure 1). Note that Cr, Sm and I denote crystal, smectic and isotropic phases, respectively.

POM of **D-3** revealed a focal conic texture characteristic of the smectic X (SmX) phase (Figure 2(a)). The XRD of **D-3** measured at 90°C gave a sharp diffraction peak in the small-angle region ($2\theta = 2.4°$), corresponding to 36.8 Å, which is ascribed to the interlayer distance. The diffraction peak in the wide-angle region ($2\theta = 18–22°$) was assigned to the intermolecular distance of LCs (from 4.9 to 4.07 Å) (Figure 3). From the POM and XRD results, the LC phase of **D-3** was assigned as being smectic.

In contrast, the phase transition temperatures of **D-9** were as follows: Cr→79°C→SmA→99°C→I and Cr←52°C←SmA←63°C←I in the heating and cooling process, respectively (Figure 1). POM of **D-9** revealed a fan-shape texture characteristic of a smectic A (SmA) phase (Figure 2b) (*14b*).

Amplification of HTP and molecular extension

The N*-LCs were prepared by adding a small amount of chiral dopant into an equimolar mixture of the N-LCs PCH302 and PCH304. The molecular structures of PCH302 and PCH304 are shown in Scheme 2. It should be noted that although each component (PCH302 or PCH304) exhibits a LC phase, the LC temperature region is very narrow, i.e. less than 1–2°C. This is not suitable for evaluating the properties of the N*-LC, because even a small change of temperature easily transforms LC phase into an isotropic one. Hence, we prepared a mixture by using two N-LCs with equimolar concentration. In the
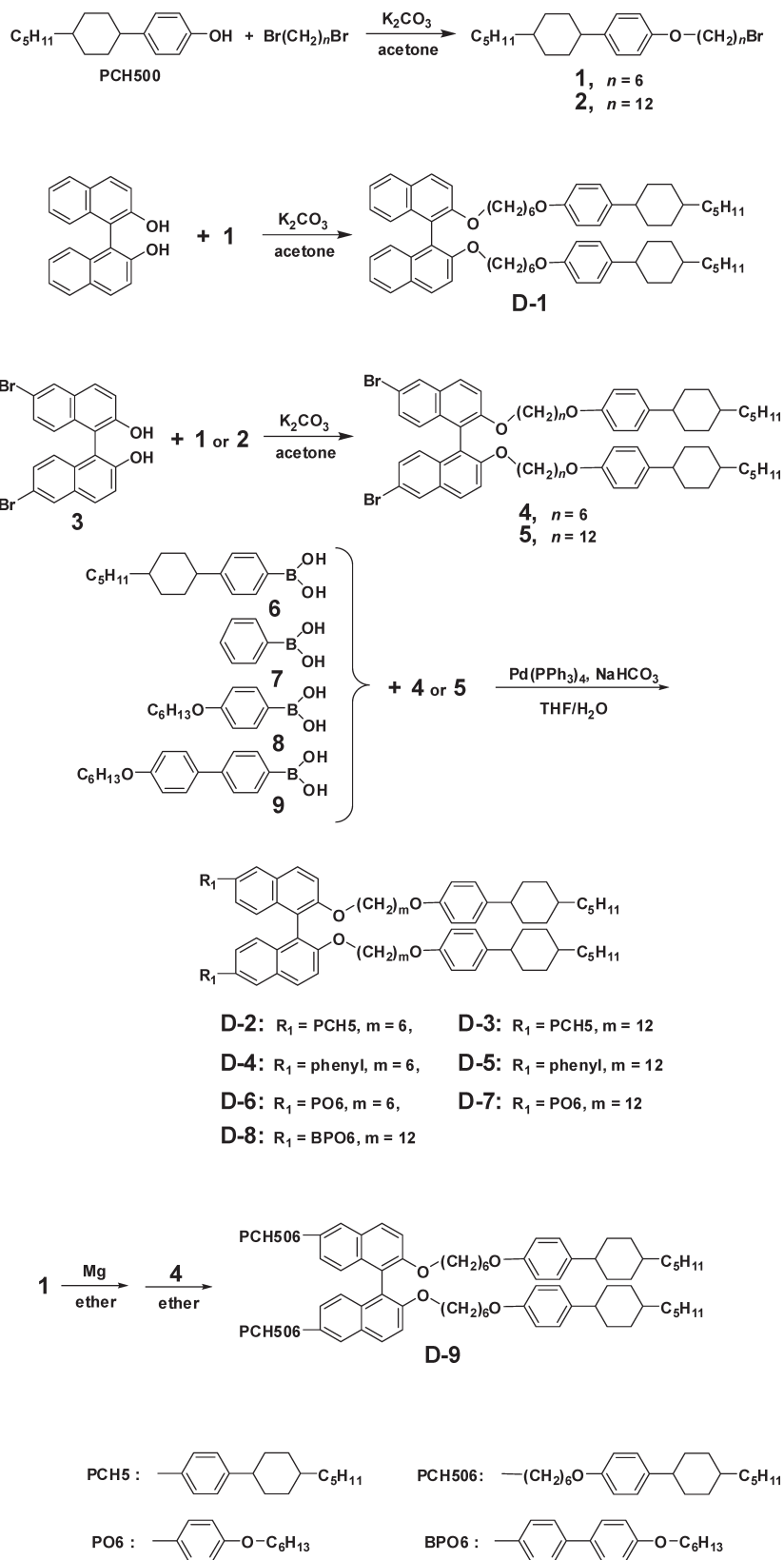
Scheme 1. Synthetic routes for di- and tetra-substituted axially chiral binaphthyl derivatives.
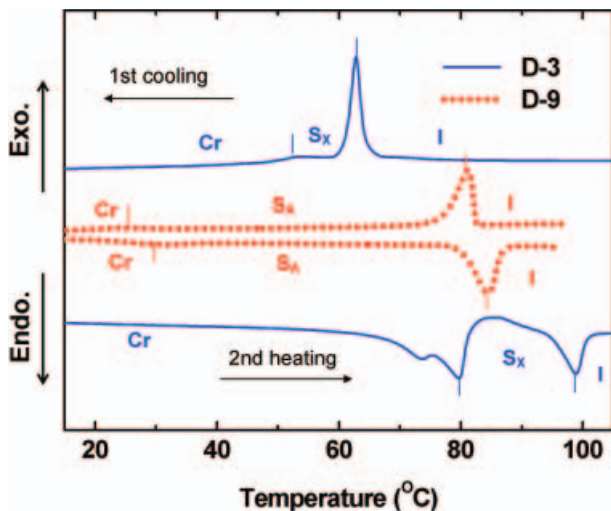
Figure 1. DSC thermographs of tetra-substituted binaphthyl derivatives, **D-3** and **D-9**.

mixture, the nematic to isotropic temperature, T_{N-I}, and the crystalline to nematic temperature, T_{C-N}, might be raised and lowered, respectively. In fact, the mixture exhibited a N-LC phase in the region from 0 to 30°C (*5, 18*).

The helical pitch of the N*-LCs was precisely evaluated by measuring the distance between Cano lines appearing on the surface of a wedge type cell under POM observation (*5c, 14b, 19*). Meanwhile, when the helical pitch was smaller than 1 μm, it was evaluated with the selective light reflection method. The helical pitch was evaluated according to the equation
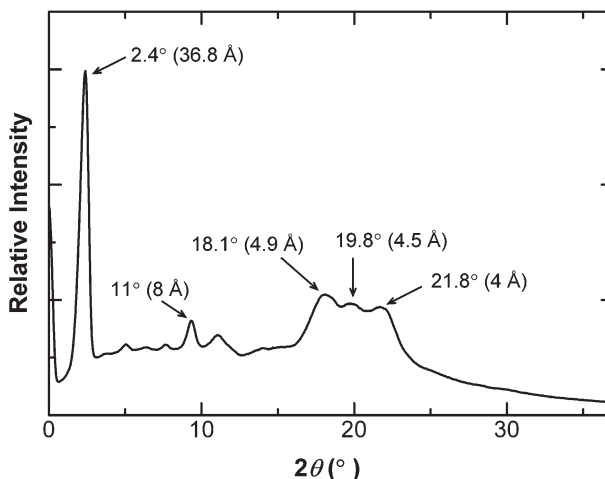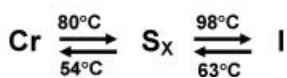
$$p = \lambda_{max}/n, \qquad (1)$$
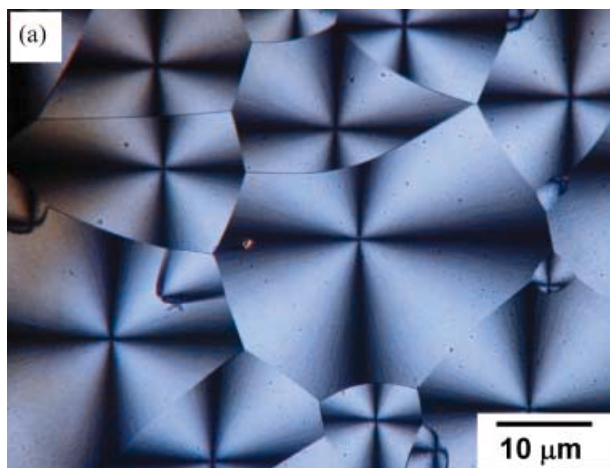
Figure 3. XRD pattern of **D-3** at 90°C in the heating process.

where λ_{max} is the wavelength for the reflected light and n is the mean refraction index of the N*-LC ($n \cong 1.5$) (*5e, 20*).

Subsequently, the HTP (β_M) of the chiral dopant, i.e. its ability to convert N-LC into N*-LC, was evaluated using the equation,

$$\beta_M = [(1/p)/c]_{c \to 0}, \qquad (2)$$

where p is the helical pitch in μm and c is the mole fraction of the chiral dopant in the N*-LC (*12, 17, 21*). We plotted the inverse of pitch ($1/p$) as a function of the mole fraction of the chiral dopant, and obtained linear relationship between $1/p$ and c in the low concentration regime.

The relationship between the number of substituents and HTP was investigated. **D-1** and **D-9** have

Figure 2. Polarising optical micrographs of **D-3** at 62°C in the cooling process (a) and **D-9** at 83°C in the heating process (b).

Host Nematic LCs

PCH302　　　**PCH304**

Scheme 2. Molecular structures of host nematic LCs, PCH302 and PCH304.
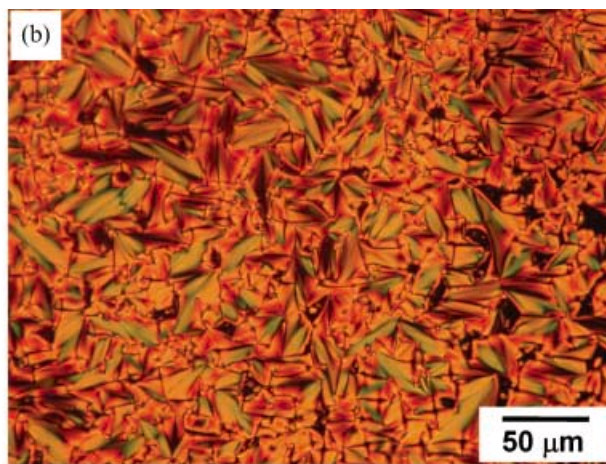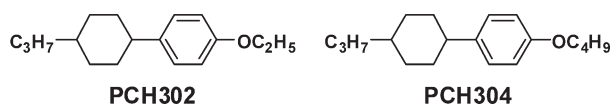
the PCH substituents at the 2,2′ positions of the binaphthyl rings but the latter (**D-9**) also has the same PCH moieties at the 6,6′ positions of the binaphthyl rings. Therefore, there was a difference between the HTPs of **D-1** ($171\,\mu m^{-1}$) and **D-9** ($200\,\mu m^{-1}$) (see Table 1). In addition, all the HTPs of the tetra-substituted chiral dopants (**D-2**–**D-9**) were larger than that of **D-1**. This may be rationalised with a difference in the number of substituents. Namely, the axially twisting torque of the tetra-substituted chiral dopants are more effectively transferred to the environmental N-LC molecules, by virtue of inter-molecular interactions between four PCH substituents and the host N-LC molecules, rather than in the case of **D-1** bearing two PCH substituents.

Interestingly, **D-3** showed a high HTP of $449\,\mu m^{-1}$, which is about 2.2 times larger than that of **D-9** ($200\,\mu m^{-1}$). The PCH moieties of **D-3** and **D-9** are linked directly and indirectly to the 6,6′ positions of the binaphthyl rings, respectively. To elucidate the relationship between the molecular structure and HTP, the equilibrium geometries of **D-3** and **D-9** are shown in Figure 4. It can be understood that absence of the hexamethylene spacer, [–$(CH_2)_6$–], in **D-3** leads to a large rigidity in the linkage between the PCH moieties and the binaphthyl rings.

When the substituent group changes from the PCH moiety (**D-3**) to phenyl (**D-5**), *p*-hexaoxyphenyl (**D-7**) and *p*-hexaoxybiphenyl (**D-8**), the HTP of these binaphthyl derivatives is changed from 449 to 183, 192 and $757\,\mu m^{-1}$, respectively. Interestingly, a close relationship between the length of aromatic group and the HTP was observed (Table 1). The molecular extension increases as follows; *p*-hexaoxybiphenyl > PCH > *p*-hexaoxyphenyl > phenyl. The HTPs increased in proportion to the molecular extension. As a result, we obtained an HTP of $757\,\mu m^{-1}$ in **D-8**, which is about four times larger than that ($183\,\mu m^{-1}$) of **D-5**.

D-3 has a rigid linkage between the 6,6′ positions of the binaphthyl rings and the PCH moieties, similar to that of **D-2**. Thus, it has a large HTP ($449\,\mu m^{-1}$), although the value is slightly smaller than that ($510\,\mu m^{-1}$) of **D-2**. The difference is due to an increase in the length of methylene spacer between the 2,2′ positions of the binaphthyl rings and the PCH moieties; The dodecamethylene spacer, [–$(CH_2)_{12}$–],

in **D-3** makes the PCH fragments at the 2,2′ positions of the binaphthyl rings more flexible than the case of **D-2**. This results in a slightly smaller twisting power than **D-2**.

Role of helical twisting power and liquid crystallinity of chiral dopant in induction of N-LC*

Since the helical pitch of the N*-LC is a primarily important index for practical use, we examined the role of the HTP and the miscibility of chiral dopant to the host N-LC in induction of N*-LC.

Figure 5 shows the helical pitch of the N*-LC as a function of mole percentage [mole of chiral dopant/ (mole of PCH302+mole of PCH304)] of the chiral dopant. Higher concentration and high HTP of the chiral dopants made the helical pitches smaller. However, the N*-LC becomes a solid through phase separation above an upper limit of concentration of the chiral dopant. In spite of the high HTP of **D-2**, its miscibility to the host N-LC is low due to its rigidity, depressing the maximum concentration to 0.25 mol. %. However, owing to the increase of the flexibility, **D-3** has liquid crystallinity itself. Then, the liquid crystallinity raises the miscibility of **D-3** to the host N-LC, giving a maximum concentration of 1.5 mol. %. Consequently, both the high HTP and the high miscibility of **D-3** allowed us to prepare highly twisted N*-LC, the helical pitch of which is of nano-order, i.e. 270 nm.

Figure 6 shows POM micrographs of the N*-LCs, which were induced by 0.05, 0.125, and 1.5 mol. % of chiral dopant (**R**)-**D-3**. Figure 6(a) and 6(b) show a fingerprint texture with striae. The distance between the striae corresponds to half of the helical pitch in the N*-LC. Meanwhile, the micrograph in Figure 6(c) shows a fan-shaped texture, but no striae were observed. This is due to the fact that the distance between the striae formed in N*-LC including 1.5 mol. % of chiral dopant (**R**)-**D-3** is too small to be detected by POM with a resolution limit of ca. 1 μm. It should be emphasised here that although the liquid crystallinity of the chiral dopant has no direct influence on the HTP, it plays an important role in increasing the miscibility of the chiral dopant, leading to an increase of the upper limit concentration usable for the chiral dopant in the host N-LC.

The phase transition temperature (clearing temperature) from N*-LC to isotropic phase depends on the molecular structure and the mole concentration of the chiral dopant, as well as the intermolecular interactions between the chiral dopant and the N-LCs (*22*). Figure 7 shows the N*-LC–isotropic phase transition temperatures of the mixed systems as a function of mole concentration of the chiral dopant.

Table 1. Comparison of rigidity, helical twisting power (HTP, β_M), and liquid crystallinity between several types of *tetra*-substituted binaphthyl derivatives (*R*-configuration)
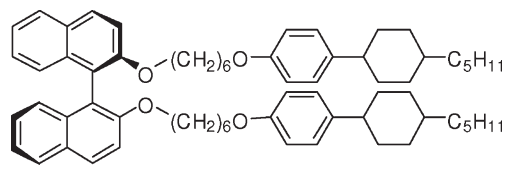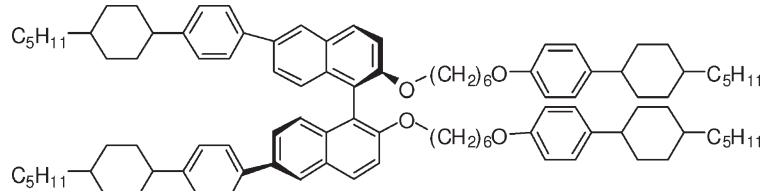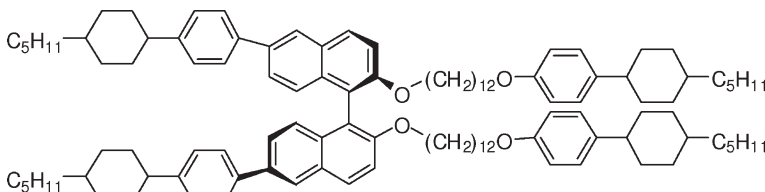
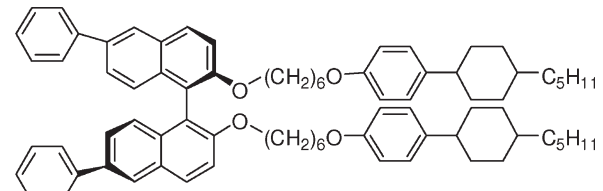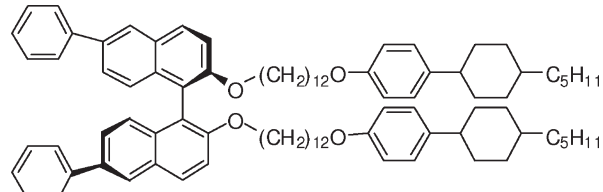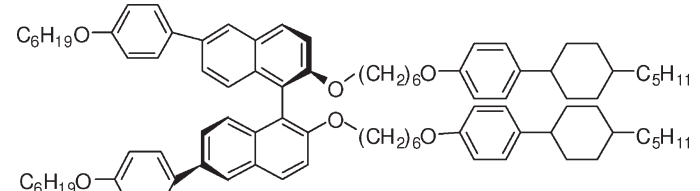|	Rigidity[a]	HTP, β_M (μm^{-1})	Liquid crystallinity[b]	Molecular structure
D-1	low	171	–	
D-2	high	510	–	
D-3	high	449	SmX	
D-4	high	226	–	
D-5	high	183	–	
D-6	high	234	–	

Table 1. (*Continued*)

	Rigidity[a]	HTP, β_M (μm^{-1})	Liquid crys-tallinity[b]	Molecular structure
D-7	high	192	–	
D-8	high	757	–	
D-9	low	200	SmA	

a) Rigidity in terms of linkages between the 6,6′ positions of the binaphthyl rings and the phenylcyclohexyl (PCH) moieties. b) Liquid crystallinity of chiral dopant itself.

Since the chiral dopants of **D-3** and **D-9** have liquid crystallinity themselves, the intermolecular interactions between the chiral dopants and the N-LCs should be larger than those in the case of **D-1** and **D-7** having no liquid crystallinity. Thus, the increases in mole concentration of **D-3** and **D-9** raise the clearing point (*23*). This suggests a thermal stability of the N*-LC phase including **D-3** or **D-9**. However, the N*-LC including **D-1** or **D-7** showed a reverse trend, i.e. a lowering of the clearing temperature with increasing the mole concentration.

We also found that the N*-LCs induced by **D-3** showed selective light reflections in the visible region, as shown in Figure 8. The reflection colour depends on the helical pitch of the N*-LC. Owing to high upper limit (1.5 mol. %) in mole concentration, we were able to adjust the helical pitches of the N*-LCs. N*-LCs with blue, green and red colours in the selective light reflection were prepared by using the chiral dopant **D-3** of 0.75, 1 and 1.5 mol. %, respectively.

The helical sense of the N*-LCs was examined through the miscibility test (*5*). The mixing area between the N*-LC and a standard LC was observed using POM. When the screw direction of the N*-LC is the same as that of the standard LC, the mixing area should be continuous. However, a discontinuous boundary (a Schlieren texture characteristic of N-LC) should appear between the N*-LC and the standard LC when they have opposite screwed directions. The cholesteryl oleyl carbonate was used as the standard LC for the miscibility test. As shown in Figure 9, a discontinuous or continuous area appeared between the N*-LC with (**R**)-**D-3** or (**S**)-**D-3** and the standard LC, respectively. Because the screw direction of the standard LC is known to be left-handed, the screw directions of the N*-LCs induced by (**R**)-**D-3** and (**S**)-**D-3** can be deduced to be opposite to and the same as that of the standard LC, i.e. right- and left-handed, respectively.

4. Conclusions

We synthesised a series of tetra-substituted binaphthyl derivatives by introducing several aromatic moieties into the 6,6′ positions of binaphthyl
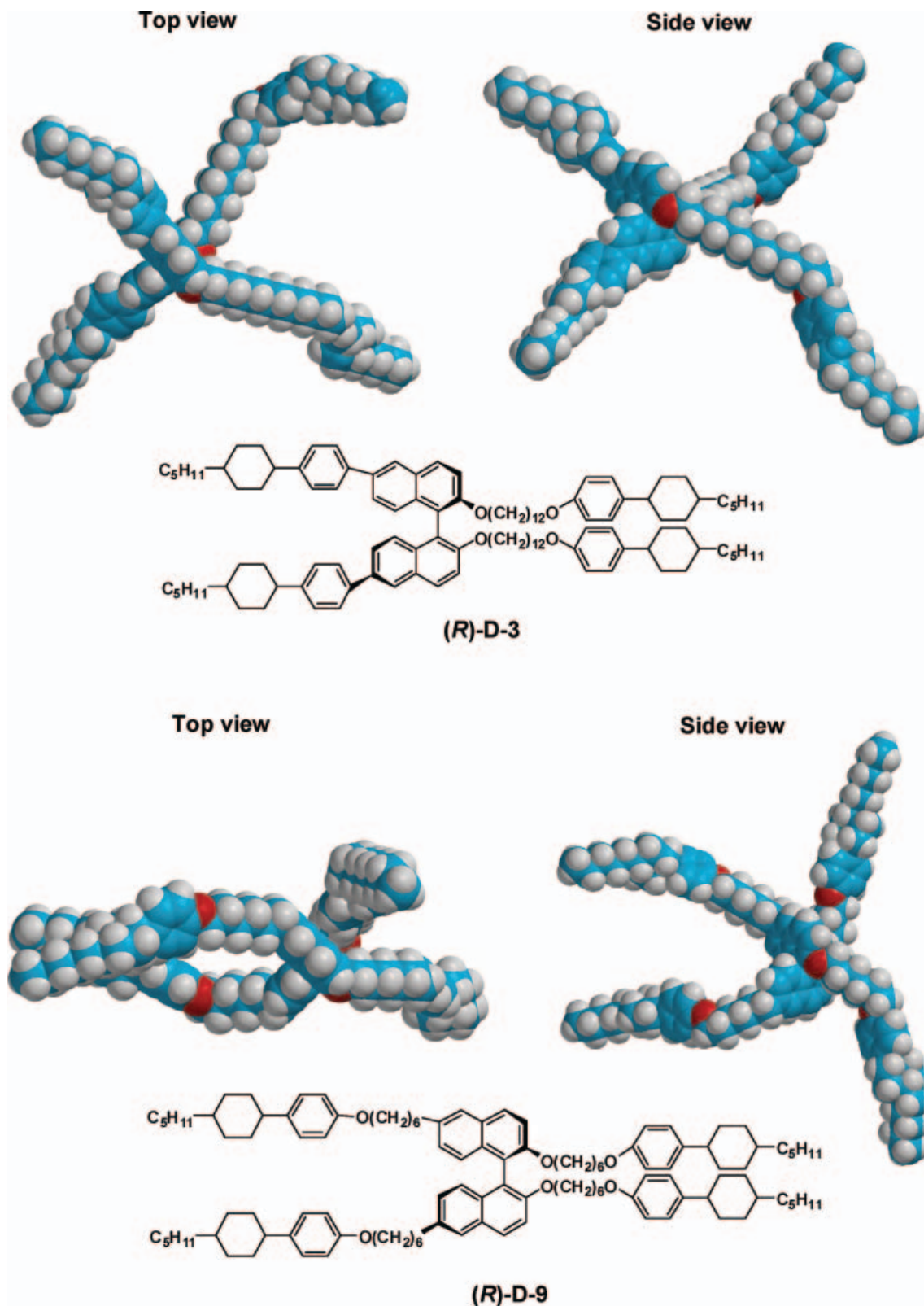
Figure 4. Three-dimensional descriptions of molecular structures of (*R*)-tetra-substituted binaphthyl derivatives, **D-3** and **D-9**. The equilibrium geometries were obtained by the semi-empirical AM1 method.
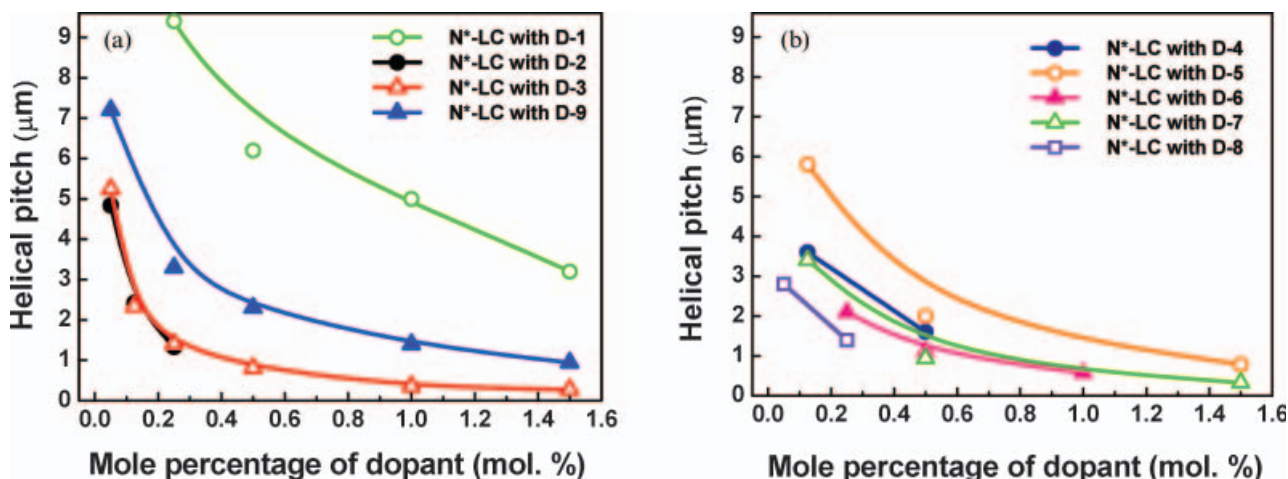
Figure 5. Changes of helical pitches in N*-LCs as a function of mole percentage of dopant (a, b). Helical pitches longer and shorter than 1 μm were evaluated by Cano's wedge method and the selective light reflection method, respectively.

rings without methylene spacers. The extremely large value of $757\,\mu m^{-1}$ in helical twisting power (HTP) for the N*-LC including the chiral dopant of **D-8** is the highest value of the axially chiral binaphthyl derivatives.

We elucidated the roles of HTP and liquid crystallinity of the chiral dopant in preparation of highly twisted N*-LCs. The HTP of $449\,\mu m^{-1}$ and liquid crystallinity of **D-3** allowed us to prepare the N*-LC with helical pitches of 850 to 270 nm by adding small amounts (0.5–1.5 mol. %) of the chiral dopant (**D-3**) into the host N-LC.

5. Syntheses

PCH506Br (1)

4-(*trans*-4-*n*-pentylcyclohexyl)phenol (PCH500, 10 g, 40 mmol) in 25 ml of acetone was added dropwise to a stirred solution of 1,6-dibromohexane (10 ml, 120 mmol), K_2CO_3 (16.5 g, 120 mmol) and a catalytic amount of 18-crown-6-ether in 300 ml of acetone for 12 h at 60°C. Subsequently, the mixture was refluxed for 24 h. The mixture was cooled, K_2CO_3 removed by filtration and washed several times with H_2O and ether. The organic layer was washed with saturated NaCl solution and dried over Na_2SO_4. The organic solvent was removed by rotary evaporation and the remaining 1,6-dibromohexane was distilled out at reduced pressure. Purification by silica gel column chromatography (*n*-hexane/CH_2Cl_2=1) and recrystallisation from ethanol afforded 14.11 g (yield = 86.2%) of white powder. ^{1}H NMR (270 MHz, CDCl$_3$): δ 0.86–1.55 (m, 20H, CH, CH$_2$, CH$_3$), 1.72–1.93 (m, 8H, CH$_2$, cyclohexane, Ph–CH–CH_2–CH$_2$–), 2.35–2.44 (m, 1H, cyclohexane, Ph–*CH*–CH$_2$–), 3.41 (t, 2H, J=6.76 Hz, Ph–O–CH_2–CH$_2$–),

3.92 (t, 2H, J=6.44 Hz, Br–CH_2–CH$_2$–), 7.08, 7.12 (d, 4H, J=2.97 Hz, Ar–H). ^{13}C NMR (270 MHz, CDCl$_3$): δ 14.5, 23.5, 25.9, 27.2, 28.9, 31.6, 32.3, 33.2, 34.3, 34.5, 35.1, 37.2, 39.8, 44.0, 65.5, 114.6, 128.1, 140.5, 157.2. Elemental analysis: calculated for C$_{23}$H$_{37}$BrO, C 67.47, H 9.11; found, C 67.21, H 9.10%.

PCH5012Br (2)

^{1}H NMR (270 MHz, CDCl$_3$): δ 0.88–1.44 (m, 32H, CH, CH$_2$, CH$_3$), 1.76–1.86 (m, 8H, CH$_2$, cyclohexane, Ph–CH–CH_2–CH$_2$–), 2.38–2.40 (m, 1H, cyclohexane, Ph–*CH*–CH$_2$–), 3.40 (t, 2H, J= 6.86 Hz, Ph–O–CH_2–CH$_2$–), 3.92 (t, 2H, J=6.55 Hz, Br–CH_2–CH$_2$–), 6.80, 7.11 (d, 4H, J=2.78 Hz, Ar–H). ^{13}C NMR (270 MHz, CDCl$_3$): δ 14.53, 23.13, 26.48, 27.08, 28.59, 28.95, 29.17, 29.77, 29.79, 29.83, 29.92, 29.93, 32.63, 33.25, 34.08, 34.43, 35.01, 37.74, 37.82, 44.15, 68.35, 114.65, 127.97, 140.33, 157.64. Elemental analysis: calculated for C$_{29}$H$_{49}$BrO, C 70.56, H 10.01; found, C 70.91, H 9.95%.

(R)-2,2′-hydroxy-6,6-Br-Binol (3)

(*R*)–2,2′–dihydroxy–1,1′–binaphthyl (3.45 g, 12.03 mmol) in 50 ml of CH$_2$Cl$_2$ was cooled to 0°C. A solution of bromine 5 g (31.28 mmol) was added slowly with stirring, keeping the temperature 0°C. Stirring was continued for 8 h at room temperature (RT. The solution was washed with NaHSO$_3$ solution, 10% NaOH and washed several times with H$_2$O and ether. The organic layer was washed with saturated NaCl solution and dried over Na$_2$SO$_4$. The organic solvent was evaporated in vacuo and the residue was purified by silica gel column chromatography (*n*-hexane/chloroform=1) and dried in vacuo to give 4.92 g (yield=92%) of white powder. ^{1}H NMR
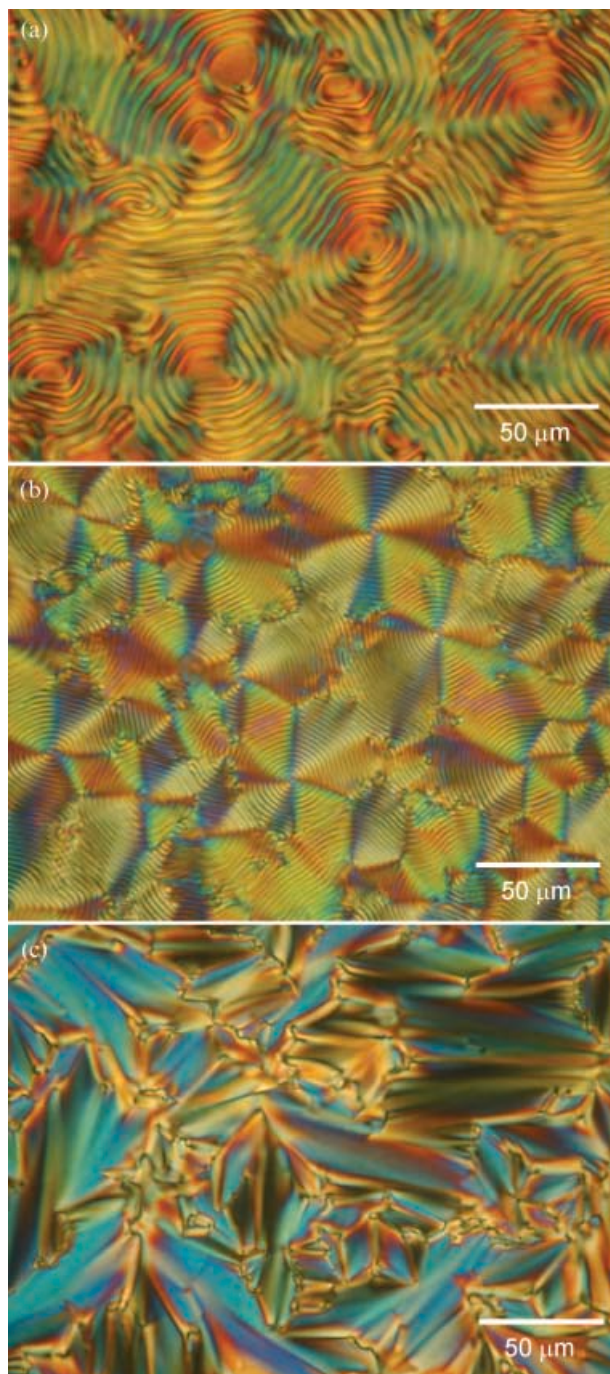
Figure 6. Polarising optical micrographs of N*-LCs at 27°C. The helical pitches of the N*-LCs are 5.3 (a), 2.3 (b), and 0.27 μm (c), respectively. The N*-LCs of (a), (b), and (c) contain 0.05, 0.125, and 1.5 mol. % of chiral dopant (**R**)-**D-3**, respectively.

(270 MHz, CDCl$_3$): δ 5.03 (s, 2H, –OH), 6.94–8.03 (m, 10H, Ar–H). ^{13}C NMR (270 MHz$_Z$, CDCl$_3$): δ 111.07, 118.42, 119.38, 126.283, 130.85, 130.97, 131.07, 131.27, 132.29, 153.36. Elemental analysis: calculated for C$_{20}$H$_{12}$Br$_2$O$_2$, C 54.09, H 2.72; found, C 54.15, H 2.92%.
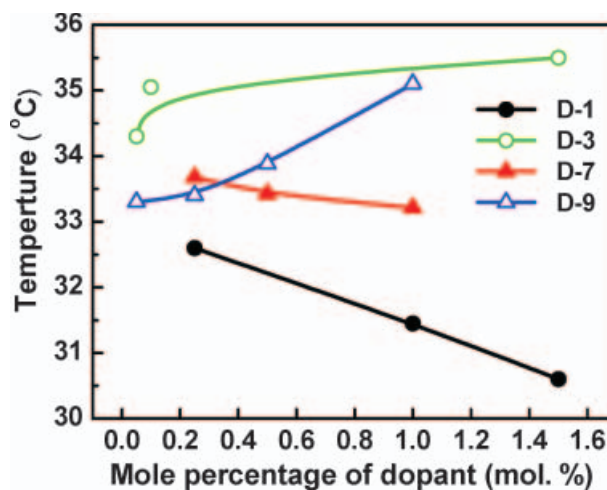
Figure 7. N*-LC–isotropic phase transition temperatures of the mixed systems (PCH302, PCH304 and dopant) as a function of mole percentage of chiral dopant (**D-1**, **D-3**, **D-7** or **D-9**). The transition temperatures of the N*-LCs were measured using DSC on cooling.

(R)-2,2′-PCH5012-6,6-Br-Binol (5)

^{1}H NMR (270 MHz, CDCl$_3$): δ 0.87–1.85 (m, 80H, CH, CH$_2$, CH$_3$), 2.36–2.40 (m, 2H, cyclohexane, Ph–*CH*–CH$_2$–), 3.87–3.96 (m, 8H, Ph–O–*CH$_2$*–CH$_2$–, Ar–O–*CH$_2$*–CH$_2$–), 6.80–7.91 (m, 18H, Ar–H). ^{13}C NMR (270 MHz, CDCl$_3$): δ 14.54, 23.08, 23.15,
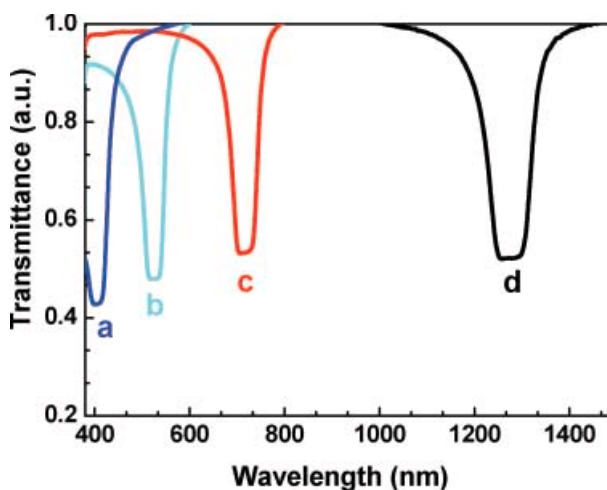
	a	b	c	d
mol. %	1.5	1.0	0.75	0.5
λ_{max}/nm	405	520	710	1270
p/nm	270	350	470	850

Figure 8. Selective light reflection spectra of N*-LCs. The N*-LCs of (a), (b), (c) and (d) contain 1.5, 1.0, 0.75, and 0.5 mol. % of chiral dopant (**R**)-**D-3**, respectively.

Figure 9. Miscibility test between the N*-LC induced by *(R)*- or *(S)*-**D-3** and the standard LC, cholesteryl oleyl carbonate of left-handed screw direction.

26.03, 26.54, 27.10, 29.56, 29.83, 29.86, 29.88, 29.89, 30.02, 32.02, 32.66, 34.11, 35.03, 37.76, 37.84, 44.17, 68.38, 70.20, 114.67, 116.31, 121.17, 123.78, 125.93, 126.41, 128.00, 128.17, 129.42, 129.68, 134.65, 140.35, 154.97, 157.67. Elemental analysis: calculated for $C_{78}H_{108}Br_2O_4$, C 73.80, H 8.57; found, C 73.52, H 8.54%.
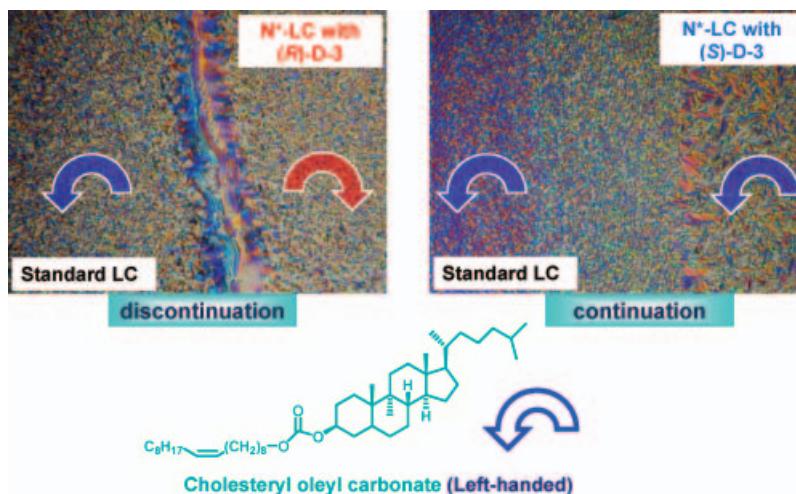
(R)-2,2′-PCH506-binaphthyl (D-1)

^{1}H NMR (CDCl$_3$): δ 0.87–1.53 (m, 48H, CH, CH$_2$, CH$_3$), 1.84–1.87 (m, 8H, cyclohexane, Ph–CH–*CH$_2$*–), 2.36–2.45 (m, 2H, cyclohexane, Ph–*CH*–CH$_2$–), 3.72 (t, 4H, J=6.42 H$_Z$, Ph–O–*CH$_2$*–CH$_2$–), 3.86–3.97 (m, 4H, Ar–O–*CH$_2$*–CH$_2$–), 6.76–7.96 (m, 20H, Ar–H). ^{13}C NMR (CDCl$_3$): δ 14.13, 22.72, 25.41, 25.47, 26.67, 29.10, 29.33, 32.22, 33.68, 34.61, 37.32, 37.41, 43.74, 67.69, 69.69, 114.25, 115.94, 120.81, 123.43, 125.48, 126.02, 127.55, 127.78, 129.06, 129.29, 134.20, 139.91, 154.50, 157.18. Elemental analysis $(C_{66}H_{86}O_4)_n$ $(943.39)_n$: calculated C 84.03, H 9.19; found C 84.08, H 9.21%. Specific rotation: $[\alpha]^{25}_{589}$= +22.5° dm^{-1} g^{-1} cm^3.

(R)-2,2′-PCH506-6,6′-PCH5-binaphthyl (D-2)

^{1}H NMR (CDCl$_3$): δ 0.87–1.52 (m, 80H, CH, CH$_2$, CH$_3$), 1.83–1.95 (m, 16H, cyclohexane, Ph–CH–*CH$_2$*–), 2.34–2.50 (m, 4H, cyclohexane, Ph–*CH*–CH$_2$–), 3.63–3.68 (t, 4H, J=6.26 Hz, Ph–O–*CH$_2$*–CH$_2$–), 3.92–3.98 (m, 4H, Ar–O–*CH$_2$*–CH$_2$–), 6.69–8.01 (m, 26H, Ar–H). ^{13}C NMR (CDCl$_3$): δ 14.23, 22.82, 25.53, 26.77, 29.21, 29.40, 32.32, 33.71, 33.76, 34.44, 34.69, 37.43, 37.49, 43.78, 44.34, 67.64, 69.78, 114.12, 116.28, 120.63, 125.29, 125.72, 125.91, 126.93, 127.16, 127.42, 129.29, 129.47, 133.17, 136.0, 138.54, 139.68, 146.57, 154.43,

157.0. Elemental analysis $(C_{100}H_{134}O_4)_n$ $(1400.13)_n$: calculated C 85.78, H 9.65; found C 86.09, H 9.67%. Specific rotation: $[\alpha]^{25}_{589}$=−50.1° dm^{-1} g^{-1} cm^3.

(R)-2,2′-PCH5012-6,6′-PCH5-binaphthyl (D-3)

^{1}H NMR (CDCl$_3$): δ 0.87–1.55 (m, 100H, CH, CH$_2$, CH$_3$), 1.69–1.77 (m, 4H, CH$_2$), 1.83–1.95 (m, 16H, cyclohexane, Ph–CH–*CH$_2$*–), 2.35–2.55 (m, 4H, cyclohexane, Ph–*CH*–CH$_2$–), 3.88–4.00 (m, 8H, Ph–O–*CH$_2$*–CH$_2$–, Ar–O–*CH$_2$*–CH$_2$–), 6.80–8.03 (m, 26H, Ar–H). ^{13}C NMR (CDCl$_3$): δ 14.24, 22.82, 25.76, 26.19, 26.76, 29.26, 29.49, 29.56, 29.65, 32.32, 33.47, 33.76, 34.44, 34.68, 37.41, 37.48, 43.79, 44.35, 67.97, 69.83, 114.16, 116.13, 120.50, 125.29, 125.67, 125.91, 126.93, 127.12, 127.47, 129.21, 129.41, 133.19, 135.90, 138.66, 139.78, 139.90, 146.54, 154.44, 157.10. Elemental analysis $(C_{112}H_{158}O_4)_n$ $(1568.45)_n$: calculated C 85.77, H 10.15; found C 85.90, H 10.22%. Specific rotation: $[\alpha]^{25}_{589}$=−43.5° dm^{-1} g^{-1} cm^3.

(S)-2,2′-PCH5012-6,6′-PCH5-binaphthyl

^{1}H NMR (CDCl$_3$) δ 0.87–1.53 (m, 100H, CH, CH$_2$, CH$_3$), 1.69–1.77 (m, 4H, CH$_2$), 1.83–1.95 (m, 16H, cyclohexane, Ph–CH–*CH$_2$*–), 2.35–2.55 (m, 4H, cyclohexane, Ph–*CH*–CH$_2$–), 3.88–4.00 (m, 8H, Ph–O–*CH$_2$*–CH$_2$–, Ar–O–*CH$_2$*–CH$_2$–), 6.80–8.03 (m, 26H, Ar–H). ^{13}C NMR (CDCl$_3$): δ 14.10, 22.70, 25.63, 26.06, 26.63, 29.13, 29.38, 29.42, 29.52, 32.18, 33.59, 33.63, 34.31, 34.55, 37.28, 37.35, 43.67, 44.22, 67.84, 69.71, 114.02, 116.00, 120.38, 125.17, 125.55, 125.78, 126.70, 127.34, 128.61, 129.10, 129.28, 133.07, 135.78, 138.54, 139.66, 141.38, 146.42, 154.31, 156.95. Elemental analysis $(C_{112}H_{158}O_4)_n$ $(1568.45)_n$: calculated C 85.77, H 10.15; found C

85.09, H 9.89%. Specific rotation: $[\alpha]^{25}_{589}=$ +30.2° dm^{-1} g^{-1} cm^3.

(R)-2,2′-PCH506-6,6′-phenyl-Binol (D-4)

^{1}H NMR (270 MHz, CDCl$_3$): δ 0.87–1.50 (m, 48H, CH, CH$_2$, CH$_3$), 1.83–1.87 (m, 8H, cyclohexane, Ph–CH–*CH$_2$*–), 2.34–2.43 (m, 2H, cyclohexane, Ph–*CH*–CH$_2$–), 3.65–3.70 (t, 4H, J=6.51 Hz, Ph–O–*CH$_2$*–CH$_2$–), 3.88–4.05 (m, 4H, Ar–O–*CH$_2$*–CH$_2$–), 6.70–8.04 (m, 28H, Ar–H). ^{13}C NMR (270 MHz, CDCl$_3$): δ 14.10, 22.68, 25.43, 26.63, 29.08, 29.27, 31.53, 32.18, 33.62, 34.56, 37.27, 37.35, 43.66, 67.49, 69.56, 113.99, 116.08, 120.35, 125.49, 125.55, 125.85, 126.74, 126.93, 127.39, 128.53, 129.26, 133.18, 135.84, 139.59, 140.90, 154.42, 156.87. $[\alpha]^{25}_{589}=$-19.36°dm^{-1}g^{-1}cm^3. Elemental analysis: calculated for C$_{78}$H$_{94}$O$_4$, C 85.51, H 8.65; found, C 85.77, H 8.73%.

(R)-2,2′-PCH5012-6,6′-phenyl-Binol (D-5)

^{1}H NMR (270 MHz, CDCl$_3$): δ 0.86–1.53 (m, 68H, CH, CH$_2$, CH$_3$), 1.68–1.76 (m, 4H, CH$_2$), 1.83–1.87 (m, 8H, cyclohexane, Ph–CH–*CH$_2$*–), 2.35–2.44 (m, 2H, cyclohexane, Ph–*CH*–CH$_2$–), 3.88–4.01 (m, 8H, Ph–O–*CH$_2$*–CH$_2$–, Ar–O–*CH$_2$*–CH$_2$–), 6.80–8.06 (m, 28H, Ar–H). ^{13}C NMR (270 MHz, CDCl$_3$): δ 141.10, 22.68, 25.65, 26.05, 26.62, 29.13, 29.37, 29.44, 29.52, 29.66, 32.17, 33.62, 34.54, 37.26, 37.35, 43.66, 67.84, 69.65, 114.03, 116.00, 118.38, 119.87, 120.27, 125.51, 125.85, 126.71, 126.94, 127.35, 128.51, 129.22, 133.21, 135.78, 139.67, 141.01, 154.44, 156.95. $[\alpha]^{25}_{589}=$-9.4°dm^{-1}g^{-1}cm^3. Elemental analysis: calculated for C$_{90}$H$_{118}$O$_4$, C 85.53, H 9.41; found, C 85.07, H 9.21%.

(R)-2,2′-PCH506-6,6′-PO6-Binol (D-6)

^{1}H NMR (270 MHz, CDCl$_3$): δ 0.77–1.53 (m, 66H, CH, CH$_2$, CH$_3$), 1.75–1.87 (m, 12H, CH$_2$, cyclohexane, Ph–CH–CH$_2$–), 2.34–2.43 (m, 2H, cyclohexane, Ph–*CH*–CH$_2$–), 3.64–3.68 (t, 4H, J=6.43 Hz, Ph–O–*CH$_2$*–CH$_2$–), 3.87–4.04 (m, 8H, Ar–O–*CH$_2$*–CH$_2$–, Ar–Ph–O–*CH$_2$*–CH$_2$–), 6.70–7.98 (m, 26H, Ar–H). ^{13}C NMR (270 MHz, CDCl$_3$): δ 14.03, 14.10, 22.59, 22.69, 25.44, 25.73, 26.64, 29.10, 29.27, 31.58, 32.19, 33.63, 34.56, 37.28, 37.36, 43.66, 67.52, 67.97, 69.67, 114.00, 114.61, 116.20, 120.52, 124.66, 125.42, 125.81, 127.29, 127.87, 129.04, 129.40, 132.83, 133.24, 135.56, 139.58, 154.22, 156.88, 158.27. $[\alpha]^{25}_{589}=$-28.47°dm^{-1}g^{-1}cm^3. Elemental analysis: calculated for C$_{90}$H$_{118}$O$_6$, C 83.41, H 9.18; found, C 83.23, H 9.11%.

(R)-2,2′-PCH5012-6,6′-PO6-Binol (D-7)

^{1}H NMR (270 MHz, CDCl$_3$): δ 0.87–1.54 (m, 86H, CH, CH$_2$, CH$_3$), 1.69–1.87 (m, 16H, CH$_2$, cyclohexane,

Ph–CH–*CH$_2$*–), 2.35–2.44 (m, 2H, cyclohexane, Ph–*CH*–CH$_2$–), 3.88–4.01 (m, 12H, Ph–O–*CH$_2$*–CH$_2$–, Ar–O–*CH$_2$*–CH$_2$–, Ar–Ph–O–*CH$_2$*–CH$_2$–), 6.80–8.00 (m, 26H, Ar–H). ^{13}C NMR (270 MHz, CDCl$_3$): δ 14.04, 14.11, 22.60, 22.70, 25.65, 25.72, 26.06, 26.63, 29.14, 29.25, 29.39, 29.45, 29.53, 31.57, 32.18, 33.63, 34.55, 37.27, 37.35, 43.66, 67.84, 67.98, 69.73, 114.03, 114.58, 116.06, 120.40, 125.39, 125.80, 127.35, 127.87, 129.33, 133.36, 135.48, 139.66, 156.95, 158.24. $[\alpha]^{25}_{589}=$-27.6°dm^{-1}g^{-1}cm^3. Elemental analysis: calculated for C$_{102}$H$_{142}$O$_6$, C 83.67, H 9.78; found, C 82.83, H 9.54%.

(R)-2,2′-PCH5012-6,6′-BPO6-Binol (D-8)

^{1}H NMR (270 MHz, CDCl$_3$): δ 0.87–1.53 (m, 96H, CH, CH$_2$, CH$_3$), 1.66–1.86 (m, 16H, CH$_2$, cyclohexane, Ph–CH–*CH$_2$*–), 2.35–2.43 (m, 2H, cyclohexane, Ph–*CH*–CH$_2$–), 3.85–4.04 (m, 12H, Ph–O–*CH$_2$*–CH$_2$–, Ar–O–*CH$_2$*–CH$_2$–, Ar–BP–O–*CH$_2$*–CH$_2$–), 6.77–8.10 (m, 34H, Ar–H). ^{13}C NMR (270 MHz, CDCl$_3$): δ 14.17, 14.23, 22.72, 22.82, 25.80, 25.85, 26.19, 26.76, 29.27, 29.37, 29.47, 29.53, 29.58, 29.67, 31.70, 32.30, 33.75, 34.67, 37.40, 37.48, 43.79, 53.44, 67.95, 68.11, 69.80, 114.15, 114.74, 116.16, 120.43, 125.40, 125.51, 126.03, 126.88, 127.33, 127.46, 127.84, 129.34, 129.41, 132.92, 133.35, 135.46, 139.32, 139.77, 154.59, 157.08, 158.61. $[\alpha]^{25}_{589}=$-52.9°dm^{-1}g^{-1}cm^3. Elemental analysis: calculated for C$_{114}$H$_{150}$O$_6$, C 84.71, H 9.35; found, C 84.66, H 9.30%.

Acknowledgement

References

(1) (a) Chen S.H.; Katsis D.; Schmid A.W.; Mastrangelo J.C.; Tsutsui T.; Blanton T.N. *Nature* **1999**, *397*, 506–508; (b) Oh-e, M.; Yokoyama, H.; Yorozuya, S.; Akagi, K.; Belkin, M.A.; Shen, Y.R. *Phys. Rev. Lett.* **2004**, *93,* 267402 (1–4).
(2) (a) Broer D.J.; Lub J.; Mol G.N. *Nature* **1995**, *378*, 467–469; (b) Hikmet, A.M.; Lub, J. *Prog. Polym. Sci.* **1996,** *21,* 1165–1209; (c) Witte, P.V.; Brehmer, M.; Lub, J. *J. Mater. Chem.* **1999,** *9,* 2087–2094; (d) Shibaev, V.; Bobrovsky, A.; Boiko, N. *Prog. Polym. Sci.* **2003,** *28,* 729–836.
(3) (a) Ozaki M.; Kasano M.; Kitasho T.; Ganzke D.; Haase W.; Yoshino K. *Adv. Matter.* **2003**, *15*, 974–977; (b) Cao, W.Y.; Munoz, A.; Palffy-Muhoray, P.; Taheri, B. *Nat Mater.* **2002,** *1,* 111–113; (c) Song, M.H.; Park, B.C.; Shin, K.C.; Ohta, T.; Tsunoda, Y.; Hoshi, H.; Takanishi, Y.; Ishikawa, K.; Watanabe, J.; Nishimura, S.; *Adv. Mater.* **2004,** *16,* 779–783; (d) Painter, O.; Lee, R.K.; Scherer, A; Yariv,

A.; O'Brien, J.D.; Dapkus, P.D.; Kim, I. *Science* **1999,** *284,* 1819–1821.

(4) (a) Saeva F.D.; Sharpe P.E.; Oline G.R. *J. Am. Chem. Soc.* **1975,** *97,* 204–205; (b) Pirkle, W.H.; Rinaldi, P.L. *J. Am. Chem. Soc.* **1977,** *99,* 3510–3511; (c) Eskenazi, C.; Nicoud, J.F.; Kagan, H.B. *J. Org. Chem.* **1979,** *44,* 995–999; (d) Nakazaki, M.; Yamamoto, K.; Fujikawa, K.; Maeda, M. *J. Chem. Soc., Chem. Commun.* 1979, 1086–1087; (e) Hibert, M.; Solladie, G. *J. Org. Chem.* **1980,** *45,* 5393–5394.

(5) (a) Akagi K.; Piao G.; Kaneko S.; Sakamaki K.; Shirakawa H.; Kyotani M. *Science* **1998,** *282,* 1683–1686; (b) Akagi, K.; Piao, G.; Kaneko, S.; Higuchi, I.; Shirakawa, H.; Kyotani, M. *Synth. Meth.* **1999,** *102,* 1406–1409; (c) Akagi, K.; Guo, S.; Mori, T.; Goh, M.; Piao, G.; Kyotani, M. *J. Am. Chem. Soc.* **2005,** *127,* 14647–14654; (d) Goh, M.J.; Kyotani, M.; Akagi, K. *Curr. Appl. Phys.* **2006,** *6,* 948–951; (e) Goh, M.; Kyotani, M.; Akagi, K. *J. Am. Chem. Soc.* **2007,** *129,* 8519–8527; (f) Goh, M.; Takayuki, M.; Kyotani, M.; Akagi, K. *Macromolecules* **2007,** *40,* 4762–4771; (g) Akagi, K. *Polym. Int.* **2007,** *56,* 1192–1199; (h) Mori, T.; Kyotani M.; Akagi, K. *Macromolecules* **2008,** *41,* 607–613.

(6) (a) Kang S.W.; Jin S.H.; Chien L.C.; Sprunt S. *Adv. Funct. Mater.* **2004,** *14,* 329–334; (b) Goto, H.; Akagi, K. *Angew. Chem. Int. Ed.* **2005,** *44,* 4322–4328; (c) Goto, H.; Akagi, K. *Macromolecules* **2005,** *38,* 1091–1098; (d) Goto, H.; Nomura, N.; Akagi, K. *J. Polym. Sci. A* **2005,** *43,* 4298–4302; (e) Goto, H.; Jeong, Y.S.; Akagi, K. *Macromol. Rapid Commun.* **2005,** *26,* 164–167; (f) Goto, H.; Akagi, K. *Chem. Mater.* **2006,** *18,* 255–262; (g) Goto, H.; Akagi, K. *J. Polym. Sci. A* **2006,** *44,* 1042–1047.

(7) (a) Coates D.; Gray G.W. *Phys. Rev. Lett.* **1973,** *45A,* 115–116; (b) Crooker, P.P. *Liq. Cryst.* **1989,** *5,* 751–775.

(8) (a) Renn S.R.; Lubensky T.C. *Phys. Rev. A.* **1988,** *38,* 2132–2147; (b) Srajer, G.; Pindak, R.; Waugh, M.A.; Goodby, J.W.; Patel, J. S. *Phys. Rev. Lett.* **1990,** *64,* 1545–1548.

(9) Gottarelli G.; Mariani P.; Spada G.P.; Samori B.; Forni A.; Solladie G.; Hibert M. *Tetrahedron* **1983,** *39,* 1337–1344.

(10) (a) Lee H.; Labes M.M. *Mol. Cryst. Liq. Cryst.* **1982,** *84,* 137–157; (b) Hatoh, H. *Mol. Cryst. Liq. Cryst. Sci. Technol. A* **1994,** *250,* 1–13; (c) Semenkova, G.P.; Kutulya, L.A.; Shkol'nikova, N.I.; Khandrimailova, T.V. *Cryst. Rep.,* **2001,** *46,* 118–125; (d) Guan, L.; Zhao, Y. *J. Mater. Chem.* **2001,** *11,* 1339–1344.

(11) Eelkema R.; Feringa B.L. *Org. Biomol. Chem.* **2006,** *4,* 3729–3745.

(12) Solladie G.; Zimmermann R. *Angew. Chem. Int. Ed.* **1984,** *23,* 348–362.

(13) (a) Bhatt J.C.; Keast S.S.; Neubert M.E.; Petschek R.C. *Liq. Cryst.* **1995,** *18,* 367–380; (b) Suchod, B.; Renault, A.; Lajzerowicz, J.; Spada, G.P. *J. Chem. Soc., Perkin Trans.* II **1992,** 1839–1844; (c) Gottarelli, G.; Hirbert, M.; Samori, B.; Solladie, G.; Spada, G.P.; Zimmermann, R. *J. Am. Chem. Soc.* **1983,** *105,* 7318–7321; (d) Gottarelli, G.; Spada, G.P.; Bartsch, R.; Solladie, G.; Zimmermann, R. *J. Org. Chem.* **1986,** *51,* 589–592; (e) Gottarelli, G.; Spada, G.P. *Mol. Cryst. Liq. Cryst.* **1985,** *123,* 377–388; (f) Rokunohe, J.; Yoshizawa, A. *J. Mater. Chem.* **2005,** *15,* 275–279; (g) Heppke, G.; Lotzsch, D.; Oestreicher, F. *Z. Naturforsch.* **1986,** *41a,* 1214–1218; (h) Li, Q.; Green, L.; Venkataraman, N.; Shiyanovskaya, I.; Khan, A.; Urbas, A.; Doane, J.W. *J. Am. Chem. Soc.* **2007,** *129,* 12908–12909.

(14) (a) Deussen H.-J.; Shibaev P.V.; Vinokur R.; Bjornholm T.; Schaumburg K.; Bechgaard K.; Shibaev V.P. *Liq. Cryst.* **1996,** *21,* 327–340; (b) Kanazawa, K.; Higuchi, I.; Akagi, K. *Mol. Cryst. Liq. Cryst.* **2001,** *364,* 825–834.

(15) Delden R.A.; Mecca T.; Rosini C.; Feringa B.L. *Chem. Eur. J.* **2004,** *10,* 61–70.

(16) (a) Kuball H.G.; Weiss B.; Beck A.K.; Seebach D. *Helv. Chim. Acta* **1997,** *80,* 2507–2514; (b) Seebach, D.; Beck, A.K.; Heckel, A. *Angew. Chem. Int. Ed.* **2001,** *40,* 92–138; (c) Neal, M.P.; Solymosi, M.; Wilson, M.R.; Earl, D.J. *J. Chem. Phys.* **2003,** *119,* 3567–3573.

(17) Kuball H.G.; Höfer T., 2000, In *Chirality in Liquid Crystals*; Kitzerow H.S., Bahr C. (Eds), Vol. 1, Chapter 3, p. 67.

(18) (a) Akagi K.; Shirakawa H.; Araya K.; Mukoh A.; Narahara T. *Polymer J.* **1987,** *19,* 185–189; (b) Akagi, K.; Katayama, S.; Shirakawa, H.; Araya, K.; Mukoh, A.; Narahara, T. *Synth. Meth.* **1987,** *17,* 241–246.

(19) (a) Grandjean F. *C. R. Acad. Sci.* **1921,** *172,* 71–74; (b) Cano, R. *Bull. Soc. Fr. Mineral.* **1968,** *91,* 20–27; (c) Heppke, G.; Oestreicher, F. *Mol. Cryst. Liq. Cryst. Lett.* **1978,** *41,* 245–249; (d) Gottarelli, G.; Samori, B.; Stremmenos, C.; Torre, G. *Tetrahedron* **1981,** *37,* 395–399.

(20) (a) Friedel G. *Annls. Phys. (Paris)* **1922,** *18,* 273; (b) Yoshida, J.; Sato, H.; Yamagishi, A.; Hoshino, N. *J. Am. Chem. Soc.* **2005,** *127,* 8453–8456.

(21) (a) Heppke G.; Oestreicher F. *Z. Naturforsch.* **1977,** *32,* 899–901; (b) Kuball, H.-G.; Heppke, G. *Liq. Cryst. Today* **1995,** *5,* 5.

(22) (a) Bauman D. *Mol. Cryst. Liq. Cryst.* **1988,** *159,* 197–218; (b) Bauman, D.; Martynski, M.T.; Mykowska, E. *Liq. Cryst.* **1995,** *18,* 607–613; (c) Deussen, H.J.; Shivaev, P.V.; Vinokur, R.; Bjornholm, T.; Schaumburg, K.; Bechgaard, K.; Shivaev, V.P. *Liq. Cryst.* **1996,** *21,* 327–340.

(23) Van Hecke G.R. *J. Phys. Chem.* **1985,** *89,* 2058–2064.